PROCEEDINGS OF SCIENCE

arXiv:1006.2342v1 [hep-ex] 11 Jun 2010

Jet cross sections in neutral current deep inelastic scattering at ZEUS and determination of α_s

Claudia Glasman*
On behalf of the ZEUS Collaboration
Universidad Autónoma de Madrid, Spain
E-mail: claudia.glasman@desy.de

The latest results on jet cross sections in neutral current deep inelastic ep scattering from the ZEUS Collaboration are presented. The new results were used to perform stringent tests of perturbative QCD and extract precise values of the strong coupling. Also, the measurements have the potential to constrain further the parton distribution functions in the proton if included in QCD fits.

XVIII International Workshop on Deep-Inelastic Scattering and Related Subjects, DIS 2010
April 19-23, 2010
Firenze, Italy

*Speaker.

© Copyright owned by the author(s) under the terms of the Creative Commons Attribution-NonCommercial-ShareAlike Licence.

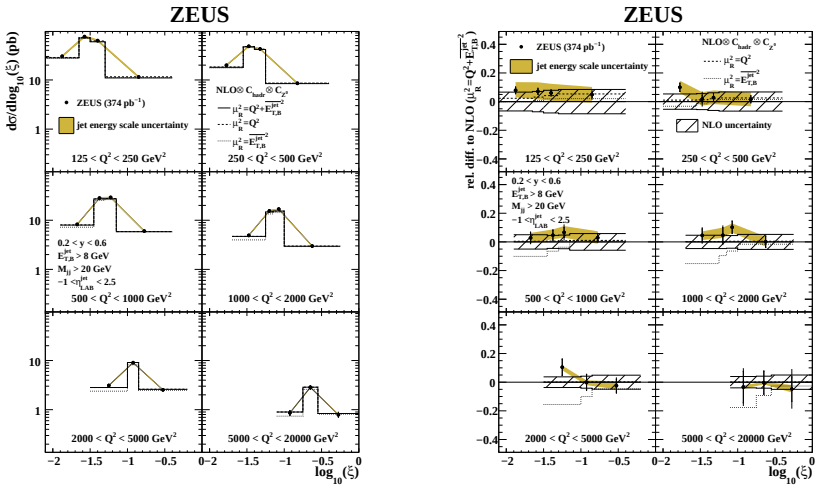

Figure 1: Dijet cross sections as functions of ξ for different regions of Q^2.

Introduction. Jet production in neutral current (NC) deep inelastic scattering (DIS) at order α_s in the Breit frame, in which the photon and the proton collide head on, proceeds via the boson-gluon fusion and QCD Compton processes. The jet production cross section can be written in perturbative QCD (pQCD) as the convolution of the parton distribution functions (PDFs) in the proton, determined from experiment, and the partonic cross sections, calculable in pQCD.

QCD processes are dominant in hadron colliders and represent a significant background to e.g. new physics searches at LHC. Measurements of jet production in NC DIS at HERA provide a clean hadron-induced reaction and a powerful tool to test pQCD calculations, determine α_s and its energy evolution. In addition, these measurements can constrain the proton PDFs, in particular the gluon density, if incorporated, together with structure function data, in the fits to extract the PDFs, as it has been done by the ZEUS Collaboration. The result was a reduction of the gluon-density uncertainty by up to a factor of two for mid- to high-x values, a region of phase space relevant for new physics searches at LHC.

The new measurements from the ZEUS experiment at HERA include inclusive-jet and dijet cross sections with more than a three-fold increase in statistics with respect to previous analyses; these data will help to constrain further the proton PDFs. The measurements were also used to perform precise tests of pQCD, extract α_s and test the performance of new jet algorithms that have recently become available.

Constraints on the proton PDFs. Measurements of dijet cross sections [1] were performed using 374 pb^{-1} of ZEUS data. The phase space of the measurement is given by photon virtualities $125 < Q^2 < 20000$ GeV^2 and inelasticity $0.2 < y < 0.6$. The jets were searched using the k_T cluster algorithm [2] in the longitudinally invariant inclusive mode [3] and selected with $E^{\rm jet}_{T,\rm B} > 8$ GeV and $-1 < \eta^{\rm jet}_{\rm LAB} < 2.5$, where $E^{\rm jet}_{T,\rm B}$ is the jet transverse energy in the Breit frame and $\eta^{\rm jet}_{\rm LAB}$ is the jet pseudorapidity in the laboratory frame. A cut on the invariant mass of the dijet system, $M^{\rm jj}$, of 20 GeV was applied to remove the regions of phase space where the pQCD calculations have limitations.

Figures 1 and 2 show the dijet cross sections as functions of $\xi = x_{\rm Bj}(1+(M^{\rm jj})^2/Q^2)$ and $\overline{E^{\rm jet}_{T,\rm B}}$, the mean transverse energy of the two jets, in different regions of Q^2, respectively. The ξ observable is an estimator of the fractional momentum carried by the struck parton. The cross

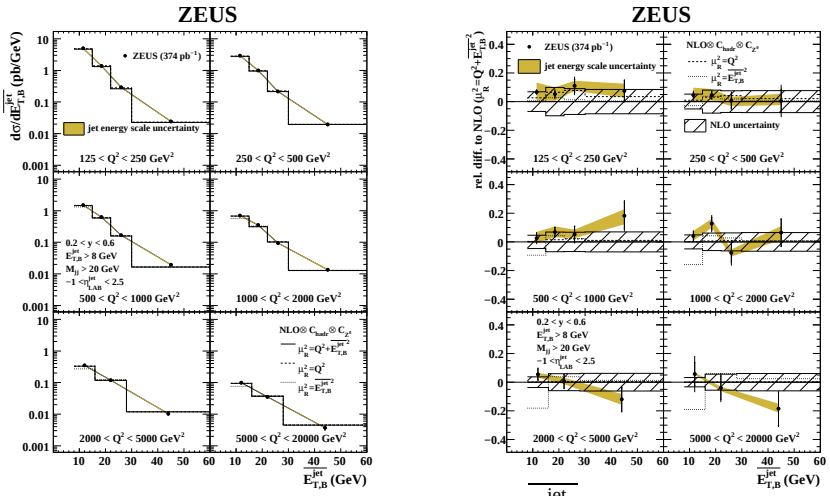

Figure 2: Dijet cross sections as functions of $\overline{E^{\rm jet}_{T,\rm B}}$ for different regions of Q^2.

section as a function of $\overline{E^{\rm jet}_{T,\rm B}}$ is well suited to make precise tests of pQCD. The measured cross sections are very precise: the uncorrelated uncertainties amount to $\sim 2\%$ at low Q^2 and $\sim 8-10\%$ at high Q^2; the jet energy scale uncertainty, which has been reduced to $\pm 1\%$, gives a contribution of ± 5 $(2)\%$ at low (high) Q^2. Next-to-leading-order (NLO) QCD predictions were computed using the program NLOJET++ [4] with renormalisation scale $\mu_R = Q^2 + (\overline{E^{\rm jet}_{T,\rm B}})^2$, factorisation scale $\mu_F = Q$ and the proton PDFs were parametrised using the CTEQ6.6 [5] sets. The predictions give a good description of the data. To ascertain the potential of the cross sections to constrain the gluon density, the predicted gluon fraction and theoretical uncertainties were studied in the phase-space region of the measurements: the predicted gluon fraction is $\sim 75\%$ at low Q^2 and decreases to $\sim 60\%$ for $Q^2 \sim 500$ GeV^2. The theoretical uncertainty due to higher orders dominates in most of the phase-space region; however, the PDF uncertainty is large in regions of phase space where the gluon fraction is still sizeable and thus the high precision dijet data presented have the potential to constrain further the proton PDFs. Similar studies were performed for inclusive-jet cross sections as functions of the $E^{\rm jet}_{T,\rm B}$ in different Q^2 regions. Also in this case the PDF uncertainty is large in regions of phase space where the gluon fraction is still sizeable.

Inclusive-jet cross sections were measured [6] using 300 pb^{-1} of ZEUS data in the kinematic region of $Q^2 > 125$ GeV^2 and $\cos\gamma_h < 0.65$. Jets were searched in the Breit frame and selected with $E^{\rm jet}_{T,\rm B} > 8$ GeV and $-2 < \eta^{\rm jet}_{\rm B} < 1.5$. Figure 3 shows the cross sections as functions of $E^{\rm jet}_{T,\rm B}$ in different regions of Q2. The measured cross sections show that the $E^{\rm jet}_{T,\rm B}$ spectrum becomes harder as Q^2 increases. These data have also small experimental uncertainties. NLO QCD calculations were computed using the program DISENT [7] with $\mu_R = E^{\rm jet}_{T,\rm B}$, $\mu_F = Q$ and the ZEUS-S [8] parametrisations of the proton PDFs. The calculations describe the data very well in the whole measured range. These measurements also have the potential to constrain further the proton PDFs.

Tests of pQCD. Single-differential inclusive-jet cross sections were measured [6] as functions of $E^{\rm jet}_{T,\rm B}$ and Q^2 to perform stringent tests of pQCD. The advantages of using inclusive-jet cross sections for performing such tests come from the fact that they are infrared insensitive (no asymmetric cuts on $E^{\rm jet}_{T,\rm B}$ or mass cuts are needed) and so a wider phase space is accessible than for dijet cross sections and they present smaller theoretical uncertainties. Also, these cross sections are suited to

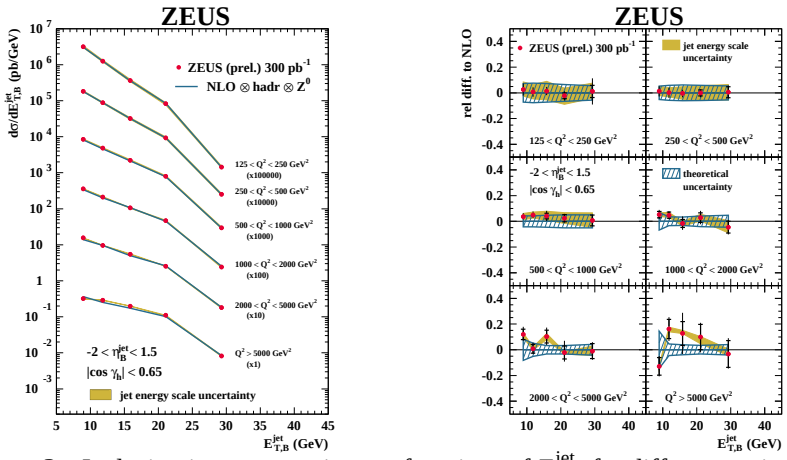

Figure 3: Inclusive-jet cross sections as functions of $E^{\text{jet}}_{T,\text{B}}$ for different regions of Q^2.

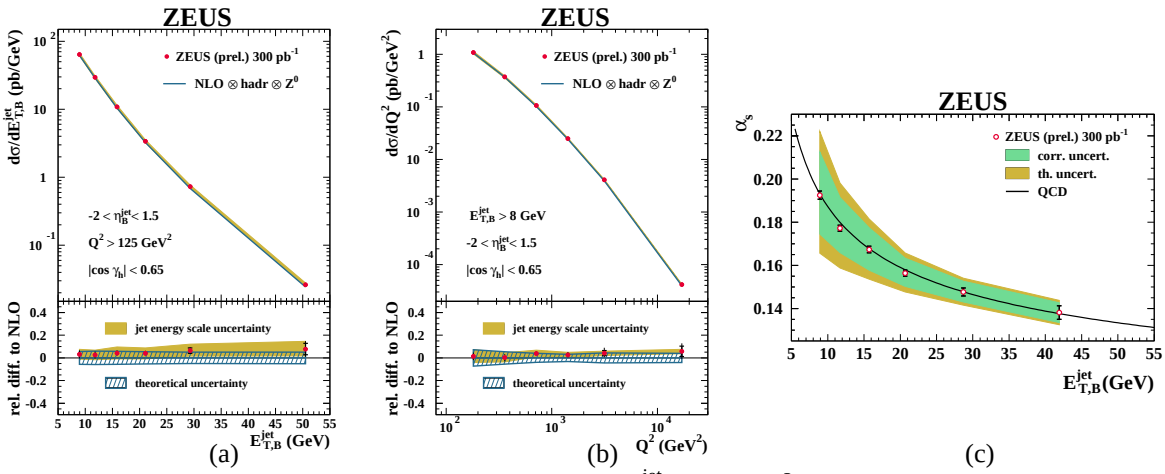

Figure 4: Inclusive-jet cross sections as functions of (a) $E^{\text{jet}}_{T,\text{B}}$ and (b) Q^2. (c) Energy-scale dependence of α_s.

test resummed calculations. Figures 4a and 4b show the cross sections as functions of $E^{\text{jet}}_{T,\text{B}}$ and Q^2, respectively. The measured cross section decreases by more than three (five) orders of magnitude within the measured range and have small experimental uncertainties. The theoretical uncertainties are also small and dominated by the terms beyond NLO; this uncertainty is smaller than 5% for $Q^2 > 250$ GeV^2. The NLO calculations describe very well both measured distributions. This demonstrates the validity of the description of the dynamics of inclusive-jet production by pQCD at order $\mathcal{O}(\alpha_s^2)$. These cross sections are directly sensitive to α_s and present small experimental and theoretical uncertainties, therefore they are particularly suited to determine this fundamental parameter.

A value of $\alpha_s(M_Z)$ was determined from a NLO QCD fit to the data for $Q^2 > 500$ GeV^2: $\alpha_s(M_Z) = 0.1208^{+0.0037}_{-0.0032}\,(\text{exp.})\,^{+0.0022}_{-0.0022}\,(\text{th.})$. In the fitting procedure, the running of α_s as predicted by QCD was assumed. The experimental uncertainties are dominated by the jet energy scale and amounts to $\pm 1.9\%$. The theoretical uncertainties are dominated by the terms beyond NLO and amounts to $\pm 1.5\%$. Other contributions to the theoretical uncertainties are: proton PDFs ($\pm 0.7\%$), hadronisation corrections ($\pm 0.8\%$) and variation of μ_F (negligible). Therefore, a very precise value of $\alpha_s(M_Z)$ was obtained from the inclusive-jet cross sections in NC DIS with a total uncertainty of

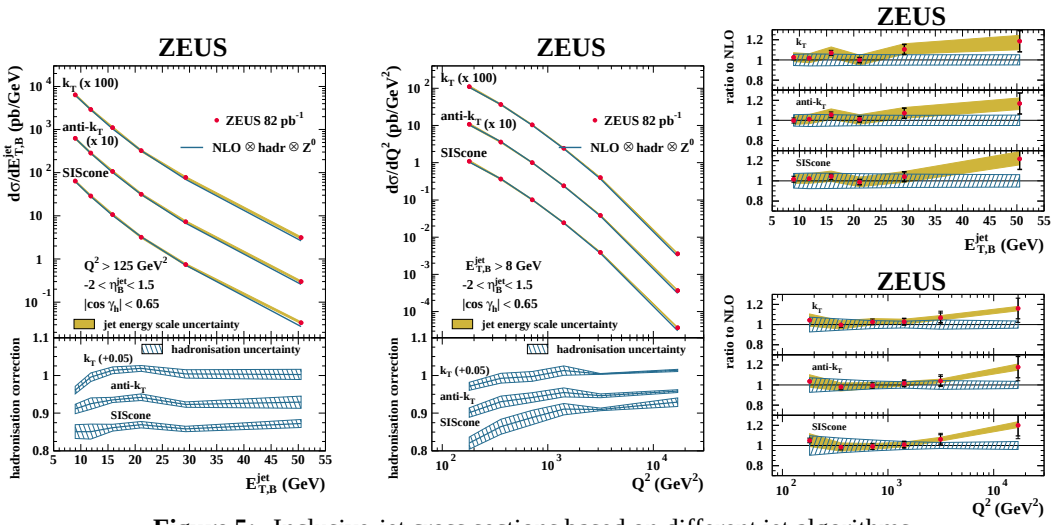

Figure 5: Inclusive-jet cross sections based on different jet algorithms.

$\sim 3.5\%$, with a contribution of only $\sim 1.9\%$ from the theoretical uncertainties. The energy-scale dependence of α_s was also determined from a NLO QCD fit to these data. Values of α_s were extracted at each mean value of $E^{\rm jet}_{T,\rm B}$ measured without assuming the running of α_s. The results are shown in Fig. 4c together with the correlated (inner band) and the theoretical (outer band) uncertainties. The black curve represents the QCD prediction for the running of α_s. The $E^{\rm jet}_{T,\rm B}$-dependence of the extracted values of α_s is in very good agreement with the predicted running of α_s over a large range in $E^{\rm jet}_{T,\rm B}$.

Testing pQCD with jets requires infrared- and collinear-safe jet algorithms. Up to now, only the k_T algorithm fulfilled these requirements at all orders. This algorithm has been tested extensively at HERA and it was proven that it has a good performance with small theoretical uncertainties and hadronisation corrections. Recently, new infrared- and collinear-safe jet algorithms, namely the anti-k_T [9] and SIScone [10], have been developed. Cluster algorithms, such as the k_T and anti-k_T jet algorithms, combine particles according to their distance in the $\eta - \phi$ plane via $d_{ij} = \min((E^i_{T,\rm B})^{2p}, (E^j_{T,\rm B})^{2p}) \cdot \Delta R^2/R^2$, in which the parameter p is set to 1 for the k_T and to -1 for the anti-k_T. The anti-k_T algorithm is also infrared and collinear safe to all orders and, contrary to the k_T, provides approximately circular jets, which is experimentally desirable to obtain stable detector corrections. The SIScone algorithm is a seedless cone algorithm and, contrary to other versions of cone algorithms, is infrared and collinear safe to all orders.

Studies [11] were performed with ZEUS data to validate these algorithms for their use in more complicated environments, such as hadron-hadron colliders. The performance of the anti-k_T and SIScone algorithms was tested in the well-understood hadron-induced NC DIS process by comparing measurements based on the new algorithms with those based on the k_T and by comparing the data and the pQCD predictions. The theoretical uncertainties for these new jet algorithms were studied and compared with those for the k_T algorithm in inclusive-jet cross sections. The uncertainties from the proton PDFs and the value of α_s are very similar for all three jet algorithms. The uncertainty from the terms beyond NLO and the modelling of the parton shower are very similar for the k_T and anti-k_T, but slightly larger for the SIScone algorithm.

The inclusive-jet cross sections were measured as functions of $E^{\rm jet}_{T,\rm B}$ and Q^2 using the three jet

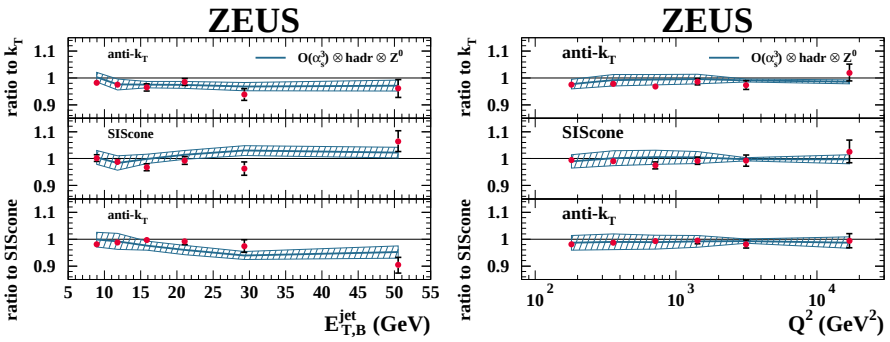

Figure 6: Ratios of cross sections based on different jet algorithms.

algorithms (see Fig. 5). The shape and normalisation of the measured and predicted cross sections are very similar; the data are very well described by the NLO calculations. The hadronisation-correction factor applied to the calculations, also shown in Fig. 5, are similar for the k_T and anti-k_T and somewhat bigger for the SIScone algorithm.

To study in more detail the performance of the new algorithms, the ratios of the cross sections between different algorithms were measured. Inclusive-jet cross sections can be calculated only up to $\mathcal{O}(\alpha_s^2)$ using the currently available programs. However, differences between cross sections using different algorithms can be calculated up to $\mathcal{O}(\alpha_s^3)$ using NLOJET++. In the case of the SIScone, differences with the k_T algorithm appear first for final states with three partons, and in the case of the anti-k_T, differences with the k_T algorithm appear first for final states with four partons. Figure 6 shows the measured ratios for anti-k_T/k_T, SIScone/k_T and anti-k_T/SIScone as functions of $E^{\text{jet}}_{T,\text{B}}$ and Q^2 together with the $\mathcal{O}(\alpha_s^3)$ predictions. The measured cross sections show differences below $\sim 3.2\%$ as a function of Q^2 and below 3.6% as a function of $E^{\text{jet}}_{T,\text{B}}$. The QCD predictions up to $\mathcal{O}(\alpha_s^3)$ give a good description of the measured ratios. The theoretical uncertainty due to higher orders of the $\mathcal{O}(\alpha_s^3)$ calculation is reduced and so the dominant uncertainty is that due to the QCD-cascade modelling. These results demonstrate the ability of the pQCD calculations including up to four partons in the final state to account adequately for the differences between the jet algorithms.

Values of $\alpha_s(M_Z)$ were extracted from the measured cross sections using the three jet algorithms. The values obtained are: $\alpha_s(M_Z) = 0.1188^{+0.0036}_{-0.0035}$ (exp.) $^{+0.0022}_{-0.0022}$ (th.) (anti-k_T), $\alpha_s(M_Z) = 0.1186^{+0.0037}_{-0.0035}$ (exp.) $^{+0.0026}_{-0.0026}$ (th.) (SIScone) and $\alpha_s(M_Z) = 0.1207^{+0.0038}_{-0.0036}$ (exp.) $^{+0.0022}_{-0.0023}$ (th.) (k_T). These determinations are consistent with each other and have a similar precision.

Summary. Figure 7a shows a summary of the values of $\alpha_s(M_Z)$ presented together with other determinations from ZEUS, both in DIS and photoproduction, and the HERA averages of 2004 [12] and 2007 [13] and the current world average [14]. The measurements are consistent with each other and the world average. The summary of the running of α_s from DIS data together with the results from photoproduction is shown in Fig. 7b. The measurements are consistent with the predicted running of α_s over a wide range of the scale. In addition, precise tests of the performance of different jet algorithms were performed. New precise jet measurements were presented which will help to constrain further the proton PDFs when included in global fits.

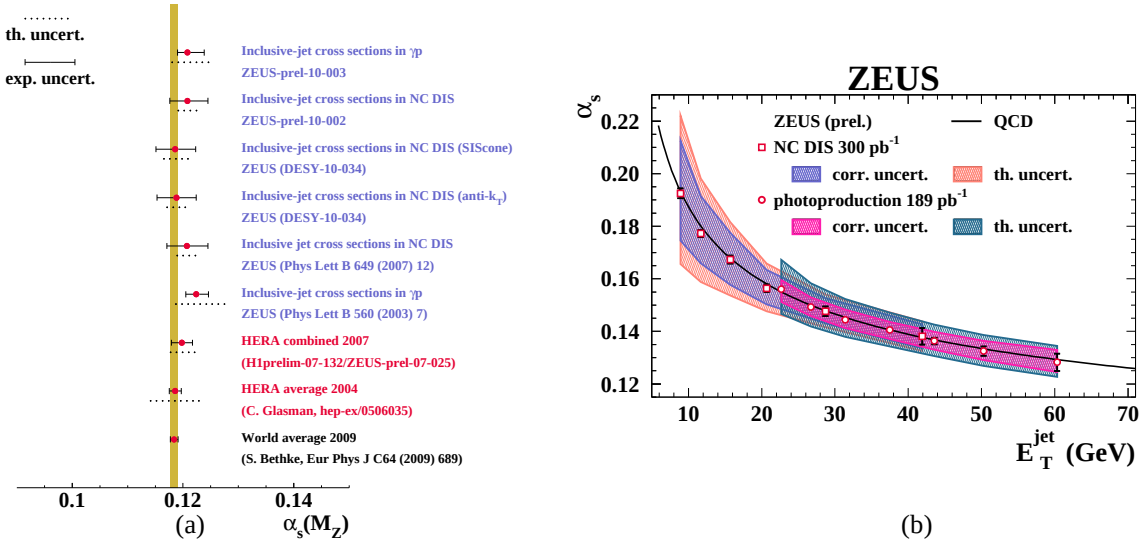

Figure 7: (a) Summary of $\alpha_s(M_Z)$ values extracted from ZEUS data together with the HERA and world averages. (b) Summary of the running α_s values extracted from ZEUS data.

References

[1] ZEUS Collaboration, H. Abramowicz et. al., ZEUS-pub-10-005.

[2] S. Catani et al., Nucl. Phys. B 406 (1993) 187.

[3] S.D. Ellis and D.E. Soper, Phys. Rev. D 48 (1993) 3160.

[4] Z. Nagy and Z. Trocsanyi, Phys. rev. Lett. 87 (2001) 082001.

[5] P. Nadolsky et. al., Phys. Rev. D 78 (2008) 013004.

[6] ZEUS Collaboration, H. Abramowicz et. al., ZEUS-prel-10-002.

[7] S. Catani and M.H. Seymour, Nucl. Phys. B 485 (1997) 291. Erratum in Nucl. Phys. B 510 (1998) 503.

[8] ZEUS Collaboration, S. Chekanov et. al., Phys. Rev. D 67 (2003) 012007.

[9] M. Cacciari, G.P. Salam and G. Soyez, JHEP 04 (2008) 063.

[10] G.P. Salam and G. Soyez, JHEP 05 (2007) 086.

[11] ZEUS Collaboration, H. Abramowicz et. al., DESY-10-034.

[12] C. Glasman, Proc. of the 13th International Workshop on Deep Inelastic Scattering, eds. S.R. Dasu and W.H. Smith, 2005, pp. 689. Also in hep-ex/0506035.

[13] C. Glasman, Proceedings of “HEP2007 International Europhysics Conference on High Energy Physics”, Manchester, England, July 2007. J. Phys. Conf. Ser. 110 (2008) 022013 Also in hep-ex/0709.4426.

[14] S. Bethke, Eur. Phys. J. C 64 (2009) 689.